JOURNAL OF AIRCRAFT
Vol. 42, No. 3, May–June 2005

Engineering Notes

ENGINEERING NOTES are short manuscripts describing new developments or important results of a preliminary nature. These Notes should not exceed 2500 words (where a figure or table counts as 200 words). Following informal review by the Editors, they may be published within a few months of the date of receipt. Style requirements are the same as for regular contributions (see inside back cover).

Extension of the *g*-Method Flutter Solution to Aeroservoelastic Stability Analysis

M. Karpel* and B. Moulin†
Technion—Israel Institute of Technology, Haifa 32000, Israel
and
P. C. Chen‡
Zona Technology, Inc., Scottsdale, Arizona, 85251

Introduction

LINEAR flutter analysis of flight vehicles is commonly based on the stability boundaries of the frequency-domain aeroelastic equation of motion in modal coordinates. Whereas the structural mass, damping, and stiffness coefficient matrices are constant in this equation, the aerodynamic influence coefficient (AIC) matrix is a transcendental function of the frequency of oscillations, calculated for required nondimensional frequency values by numerical procedures such as the doublet-lattice method[1] and the harmonic gradient method.[2] Consequently, frequency-domain flutter solvers are based on search algorithms that iterate between the system eigenvalues and the AIC matrix.

A widely adopted method for flutter solution is the *p–k* method that was first introduced by Irwin and Guyett[3] and has been generalized and modified to include a determinant-based search process by Hassig.[4] Rodden et al.[5] added a damping-dependent aerodynamic term that improved the search process. Rodden[6] introduced the *p–k* method to MSC/NASTRAN with a lining-up procedure that matched the frequency values with the imaginary parts of the resulting eigenvalues. Chen[7] extended the *p–k* concepts in the damping-perturbation g method that includes a first-order damping term that is rigorously derived from the Laplace-domain aerodynamics. Whereas the *p–k* solver searches for one aeroelastic root per each modal coordinate taken into account, the g-solver search algorithm is capable of handling extra roots due to unsteady aerodynamic lags.

Aeroservoelasticity (ASE) deals with the interaction of aeroelastic and control systems. The application of modern control design techniques requires the aeroservoelastic equations of motion to be cast in a first-order, time-domain (state-space) form. This representation requires the aerodynamic matrices to be approximated by rational functions in the complex Laplace domain (see Refs. 8 and 9). The resulting state-space equations can be easily augmented by standard control system models to provide ASE constant coefficient equations for which stability analysis is based on standard eigenvalue extraction routines, as is utilized in the ZAERO code.[10] The problem is that the aerodynamic approximation is sometimes of questionable accuracy. Hence, it is desirable to be able to perform closed-loop flutter analysis in the frequency domain, with the original tabulated AIC matrices.

ASE Equations of Motion

The Laplace transform of the open-loop aeroelastic equation of motion in modal coordinates, excited by control surface deflections, is

$$\left([M_{hh}]s^2 + [B_{hh}]s + [K_{hh}] + q[Q_{hh}(s)]\right)\{\xi(s)\} = -\left([M_{hc}]s^2 + q[Q_{hc}(s)]\right)\{\delta(s)\} \tag{1}$$

where $\{\xi\}$ and $\{\delta\}$ are the vectors of generalized structural displacements and control surface deflection commands; $[M_{hh}]$, $[B_{hh}]$, $[K_{hh}]$, and $[Q_{hh}]$ are the generalized mass, damping, stiffness, and AIC matrices; $[M_{hc}]$ and $[Q_{hc}]$ are control-coupling mass and aerodynamic matrices; s is the Laplace variable; and q is the dynamic pressure. The AIC matrices $[Q_{hh}(s)]$ and $[Q_{hc}(s)]$ can be calculated by unsteady aerodynamic codes at various tabulated reduced-frequency k values along the imaginary axis of the nondimensional Laplace variable

$$p \equiv sb/V = g + ik \tag{2}$$

where b is a reference semichord, V is the air velocity, and $k = \omega b/V$ where ω is the vibration frequency. The ASE loop can be closed by relating the input commands to the generalized displacements by

$$\{\delta\} = [T_{ch}(s)]\{\xi\} \tag{3}$$

where $[T_{ch}(s)]$ is a matrix of control transfer functions. The substitution of Eq. (3) into Eq. (1) yields

$$\left([M_{hh}]s^2 + [B_{hh}]s + [K_{hh}] + q[\bar{Q}_{hh}(s)]\right)\{\xi(s)\} = 0 \tag{4}$$

where

$$[\bar{Q}_{hh}(s)] = [Q_{hh}(s)] + \left([M_{hc}]s^2 + q[Q_{hc}(s)]\right)[T_{ch}] \tag{5}$$

Previous applications of frequency-domain schemes to closed-loop ASE systems, such as in Refs. 6 and 11, simply applied the search algorithm to $[\bar{Q}_{hh}(ik)]$ of Eq. (5) (with s replaced by ikV/b) instead of $[Q_{hh}(ik)]$. The problem is that $[\bar{Q}_{hh}(ik)]$ may yield many roots associated with those of the control system. Consequently, the search algorithm, which is looking only for n_h roots, might lose important aeroservoelastic roots. The g method provides a convenient solution to this problem.

Presented as Paper 2003-1512 at the AIAA/ASME/ASCE/AHS/ASC Structures, Structural Dynamics and Materials Conference, Norfolk, VA, 7–10 April 2003; received 6 May 2004; revision received 22 July 2004; accepted for publication 22 July 2004.

*Professor, Sanford Kaplan Chair in Aerospace Engineering. Associate Fellow AIAA.
†Senior Researcher, Faculty of Aerospace Engineering. Member AIAA.
‡Vice President. Member AIAA.

State-Space Equations with Transcendental Aeromatrices

The ASE module in the ZAERO code[10] is based on modeling the ASE problem in a constant-coefficient state-space form based on a rational approximation of the AIC matrices.[9] The control part of the modeling process transforms control components of the most general architecture into a single state-space equation that augments to the aeroelastic system. To facilitate the application of the frequency-domain g-method flutter procedure to control-augmented systems, the state-space ASE equations are expressed in this section in the Laplace domain, with the aerodynamic coefficient matrices kept in their transcendental form, before rational approximations are made. These equations can be used for s-domain stability and response analyses where the aerodynamic coefficients are interpolated from a database of force coefficient matrices calculated at tabulated reduced-frequency values. Such analyses may be useful when the rational aerodynamic approximations are of questionable accuracy, or when the results are to be compared with those obtained by other numerical solutions with interpolated aerodynamics.

The open-loop ASE equations of motion (1) and the control equation (3) can be expressed in an uncoupled form

$$s\begin{Bmatrix} x_p \\ x_c \end{Bmatrix} = \begin{bmatrix} A_p(s) & 0 \\ 0 & A_c \end{bmatrix}\begin{Bmatrix} x_p \\ x_c \end{Bmatrix} + \begin{bmatrix} B_p & 0 \\ 0 & B_c \end{bmatrix}\begin{Bmatrix} u_p \\ u_c \end{Bmatrix}$$

$$\begin{Bmatrix} y_p \\ y_c \end{Bmatrix} = \begin{bmatrix} C_p(s) & 0 \\ 0 & C_c \end{bmatrix}\begin{Bmatrix} x_p \\ x_c \end{Bmatrix} + \begin{bmatrix} 0 & 0 \\ 0 & D_c \end{bmatrix}\begin{Bmatrix} u_p \\ u_c \end{Bmatrix} \tag{6}$$

where $\{x_p\}$ and $\{x_c\}$ are the plant and the control-system state vectors. The coefficient matrices are similar to those of the regular ASE modeling process,[9,10] except that the aerodynamic terms in $[A_p]$ and $[C_p]$ retain their transcendental dependency on s. The plant state vector includes the model displacements and velocities $\{\xi\}$ and $s\{\xi\}$ and three states for each actuator, $\{\delta\}$, $s\{\delta\}$, and $s^2\{\delta\}$. The plant system matrix $[A_p(s)]$ is

$$[A_p(s)] = [A_{na}] - q[A_1][Q_{hh}(s) \quad 0 \quad Q_{hc}(s) \quad 0 \quad 0] \tag{7}$$

where $[A_{na}]$ is the plant system matrix with the aerodynamic terms ignored, which is independent of s, and where $[A_1]^T = [0 \;\; M_{hh}^{-1} \;\; 0 \;\; 0 \;\; 0]$.

The plant output matrix $[C_p(s)]$ is

$$[C_p(s)] = [C_{na}] - q[\phi_{\text{acc}}]\big[M_{hh}^{-1}\big][Q_{hh}(s) \quad 0 \quad Q_{hc}(s) \quad 0 \quad 0] \tag{8}$$

where $[C_{na}]$ is the output matrix with the aerodynamic terms ignored and $[\phi_{\text{acc}}]$ is a zero matrix except for modal displacement rows associated with acceleration outputs. The constant matrices $[A_{na}]$ and $[C_{na}]$ can be generated by the regular modeling process of Ref. 10, with the aerodynamic terms ignored. The ASE loop is closed by applying the gain matrix

$$\begin{Bmatrix} u_p \\ u_c \end{Bmatrix} = \begin{bmatrix} G_{pp} & G_{pc} \\ G_{cp} & G_{cc} \end{bmatrix}\begin{Bmatrix} y_p \\ y_c \end{Bmatrix} \tag{9}$$

The resulting closed-loop equation is

$$s\{X\} = [\bar{A}(s)]\{X\} \tag{10}$$

where $\{X\}^T = \lfloor x_p^T \;\; x_c^T \rfloor$ and

$$[\bar{A}(s)] = [\bar{A}_{na}] - q[A_2][Q_{hh}(s) \quad 0 \quad Q_{hc}(s) \quad 0 \quad 0 \quad 0] \tag{11}$$

where $[\bar{A}_{na}]$ is the closed-loop system matrix with the aerodynamic terms ignored and

$$[A_2] = \begin{bmatrix} A_1 \\ 0 \end{bmatrix} + \begin{bmatrix} B_pG_{pp} + B_pG_{pc}(I - D_cG_{cc})^{-1}D_cG_{cp} \\ B_cG_{cp} + B_cG_{cc}(I - D_cG_{cc})^{-1}D_cG_{cp} \end{bmatrix}\big[\phi_{\text{acc}}M_{hh}^{-1}\big] \tag{12}$$

Equation (11) shows that the Laplace-domain unsteady aerodynamics $[Q_{hh}(s)]$ and $[Q_{hc}(s)]$ are required to obtain the system matrix of Eq. (10). However, they cannot be generated by the frequency-domain unsteady aerodynamic method, that is, only $[Q_{hh}(ik)]$ and $[Q_{hc}(ik)]$ are available. The replacement of $[Q_{hh}(s)]$ and $[Q_{hc}(s)]$ by $[Q_{hh}(ik)]$ and $[Q_{hc}(ik)]$ is theoretically incorrect because the latter are derived from the simple harmonic motion and are valid only at $g = 0$.

Based on the premise that the Laplace-domain unsteady aerodynamics are analytic, Chen[7] showed that a first-order damping term can be rigorously obtained from the frequency-domain aerodynamics using a damping perturbation method. This led to the g method for the open-loop stability analysis. However, in this Note we will show that the g method can be expanded for the closed-loop stability analysis as well.

To apply the g method for flutter analysis, we should substitute in Eq. (10) $s = (g + ik)V/b$ and approximate $[\bar{A}(s)]$ by

$$[\bar{A}(s)] \approx [\bar{A}(ik)] + g\frac{\partial[\bar{A}(ik)]}{\partial(ik)} \tag{13}$$

which yields

$$g\{X\} = \frac{b}{V}\left([\bar{A}(ik)] + g\frac{\partial[\bar{A}(ik)]}{\partial(ik)}\right)\{X\} - ik\{X\} \tag{14}$$

The resulting eigenvalue problem for g is

$$([D] - g[I])\{X\} = 0 \tag{15}$$

where

$$[D] = \left[[I] - \frac{b}{V}\frac{\partial[\bar{A}(ik)]}{\partial(ik)}\right]^{-1}\left(\frac{b}{V}[\bar{A}(ik)] - ik[I]\right) \tag{16}$$

The topology of $[A_2]$ in Eq. (12) is such that the first and third block rows, namely, those associated with ξ and δ of $\{x_p\}$ in Eq. (6), are all zero. Equation (11) and the topology of $[A_2]$ imply that

$$\left[[I] - \frac{b}{V}\frac{\partial[\bar{A}(ik)]}{\partial(ik)}\right]^{-1} = [I] + \frac{b}{V}\frac{\partial[\bar{A}(ik)]}{\partial(ik)} = [I] - \frac{qb}{V}[A_2]$$

$$\times\left[\frac{\partial Q_{hh}(ik)}{\partial(ik)} \quad 0 \quad \frac{\partial Q_{hc}(ik)}{\partial(ik)} \quad 0 \quad 0 \quad 0\right] \tag{17}$$

Equation (15) forms the basis for application of the g method[7] that utilizes a reduced-frequency sweep technique to search for the roots of the flutter solution and a predictor–corrector scheme to ensure the robustness of the sweep technique. The frequency sweep yields the frequency-damping pairs for which the damping is real valued. The inclusion of the control states in Eq. (15) eliminates the problem of lost roots discussed earlier.

The g procedure was designed to extract modal frequency and damping values for user-defined velocity–density pairs at a certain Mach number, and to interpolate the results for the flutter boundary conditions. The procedure can also be applied to cases where the flight conditions are fixed at design values and the control gains are changed, one at a time, by multiplying them by factors or shifting them by phases. The resulting root loci can then be interpolated for traditional control gain and phase margins.

Numerical Example

Aeroelastic Model

The advanced fighter aluminum (AFA) generic aircraft model is used for the sample application. The NASTRAN aircraft structural model is shown in Fig. 1. This study is performed with antisymmetric boundary conditions, with 27 modes including one rigid-body mode in roll.

ZAERO unsteady aerodynamic model is shown in Fig. 2. The model consists of nine aerodynamic panels representing the fuselage, inboard and outboard parts of the wing, four control surfaces, tip missile, and horizontal tail. The panels representing the fuselage and the horizontal tail are attached to the support grid point of the structural model. Four root boxes of the inboard leading-edge flap panel are also attached to this point. Wing, control surfaces, and missile panels are splined to the grid points.

Roll Control System

A control system was designed to obtain a required aircraft roll-rate performance requirement subject to control deflections limits and low-frequency stability requirements.

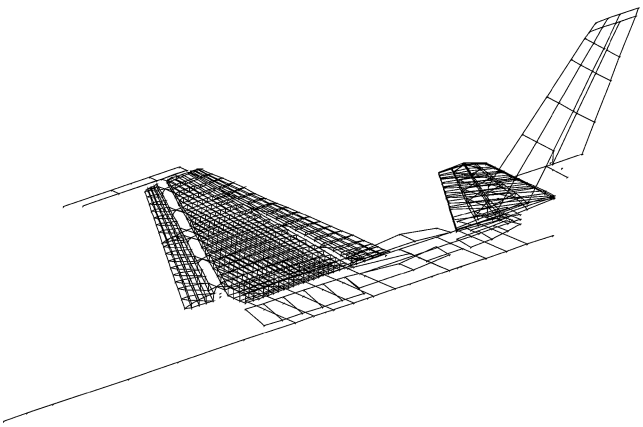

Fig. 1 AFA structural model.

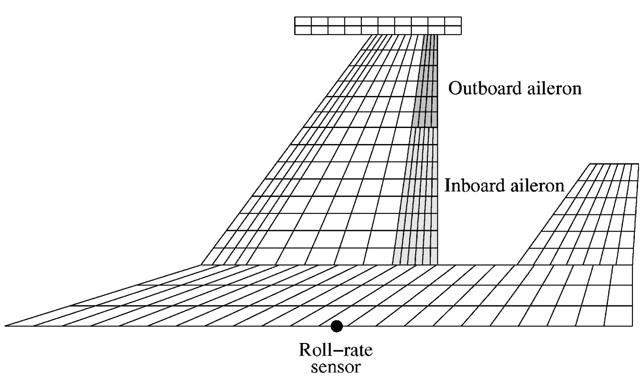

Fig. 2 AFA aerodynamic model.

The system is controlled by moving the wing trailing-edge outboard (index = 1) and inboard (index = 2) control surfaces, activated by third-order actuators with the transfer function

$$\delta/u_p = A_0 \Big/ \left(s^3 + A_2 s^2 + A_1 s + A_0\right) \tag{18}$$

The plant inputs are the actuator input commands u_{p_1} and u_{p_2}. The only output y_p is a roll-rate reading near the fuselage centerplane. It is assumed that the rate-gyro dynamics are negligible (namely, perfect measurement).

The designed roll controller contains a low-pass filter and three phase-lead compensators connected in series to the rate gyro, as well as two gains that separate the commands given to the actuators. The gains are

$$G_1 = -0.45, \qquad G_2 = 0.06 \tag{19}$$

The low-pass filter is

$$T_f = \omega_f/(s + \omega_f) \tag{20}$$

with $\omega_f = 4.0$ rad/s. The filter was designed to avoid control interaction with the structural modes, but it causes low-frequency phase-margin problems. To achieve the required phase margins, three phase-lead compensators were added of the type

$$T_{\text{plc}} = \frac{1 + s/\omega_0}{1 + s/\omega_p} = \frac{(\omega_p/\omega_0)s + \omega_p}{s + \omega_p} \tag{21}$$

with the three ω_0 values equal to 15.3, 17.0, and 18.7 rad/s and $\omega_p/\omega_0 = 1.8$ in all three cases. The roll control gains and filters accumulate to a fourth-order control system.

ASE Stability Analysis with Nominal Roll Control

Antisymmetric close-loop flutter analysis was performed at Mach 0.9. All 27 low-frequency modes, including 1 rigid-body mode, were used. There were 14 reduced-frequency values between $k = 0$ and 0.3 used to create the aerodynamic database. There were 20 flutter computation points defined at a fixed velocity of $V = 12{,}057$ in./s, with variable air density values that imply the dynamic pressure range from 0 to 10 psi. Structural damping of $g_s = 0.02$ was assumed.

The g-method variations of modal frequencies and damping values, associated with the structural modes up to 40 Hz, with q, are shown in Fig. 3. For comparison, the same flutter case was calculated

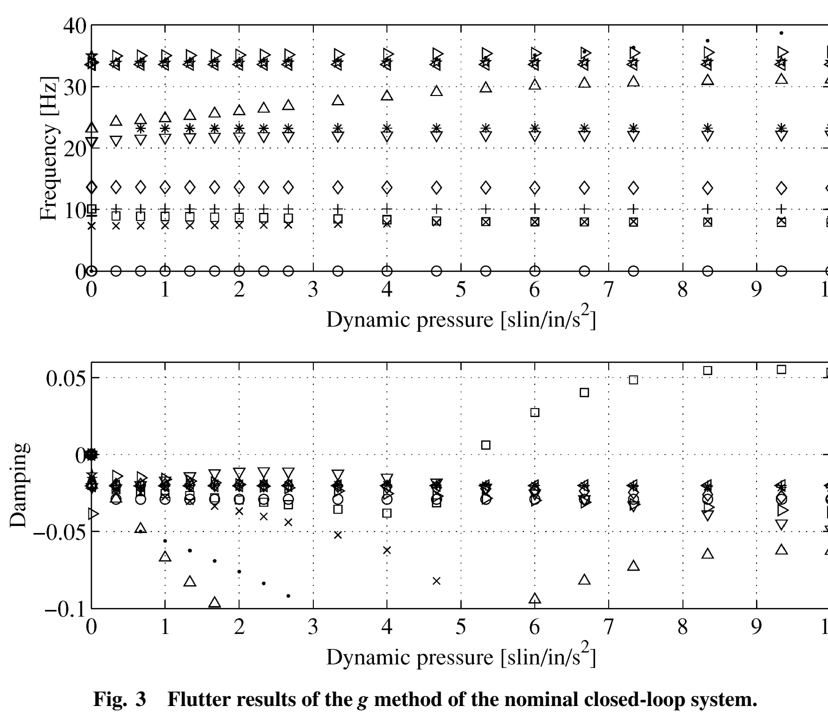

Fig. 3 Flutter results of the *g* method of the nominal closed-loop system.

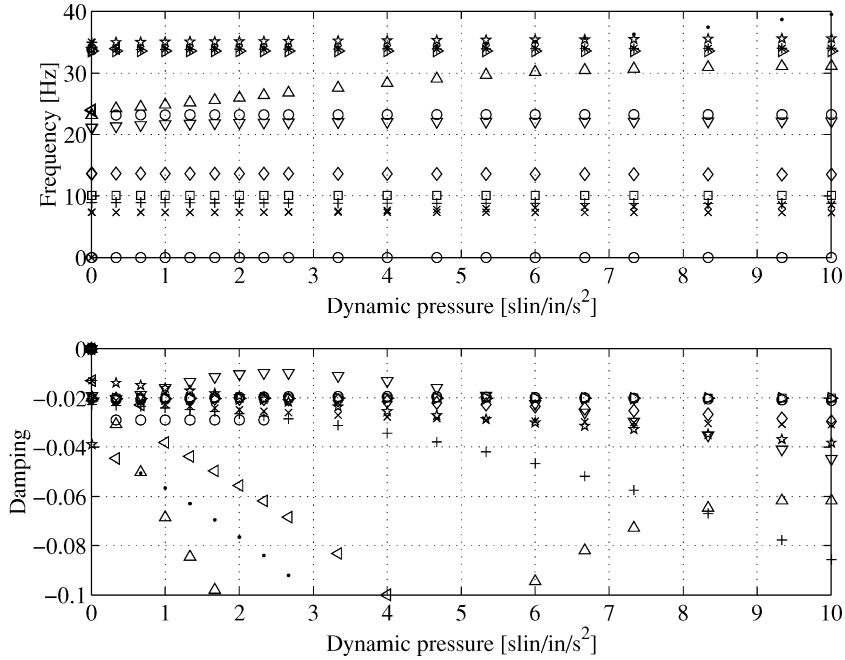

Fig. 4 Results of the *g* method of ASE system with notch filter.

using a full state-space ASE modeling based on a rational approximation of the AIC matrices. The minimum-state approximation method[9] was used with 10 aerodynamic lags, matched constraints at $k = 0$, and physical weighting of the aerodynamic data. The state-space ASE results are similar to the g-method results shown in Fig. 3.

ASE Stability Analysis with a Notch Filter

To demonstrate the application of the ASE stability analysis in a control design process, a notch filter was added to solve the ASE stability problem. The filter is used to reduce the actuator commands around flutter frequency, where the first two structural modes amplify the control system output signal. The notch filter was located between the output of the plant (sensor) and the input of the control system. The transfer function of the notch filter is of the form

$$T_{\text{nf}} = \frac{as^2 - b_1 s + 1}{as^2 - b_2 s + 1} \tag{22}$$

with $a = 4.034 \times 10^{-4}$, $b_1 = 4.034 \times 10^{-3}$ and $b_2 = 1.227 \times 10^{-2}$.

The flutter results of the ASE system with the notch filter using the g method and the state-space approach are practically identical and indicate no flutter. The g-method results are shown in Fig. 4.

Conclusions

The g-method flutter solution was modified and expanded to allow a full representation of linear control systems. All of the structural, actuator, and control states are explicitly included in the state vector of the g-method formulation. Thus, stability solutions of all states can be captured by the g method. Control systems of the most general form are represented in their full state-space realization. The g method provides an accurate damping solution that can be considered as a reference solution to verify the accuracy of rational-function aerodynamic approximations.

References

[1] Albano, E., and Rodden, W. P., "Doublet-Lattice Method for Calculating Lift Distributions on Oscillating Surfaces in Subsonic Flows," *AIAA Journal*, Vol. 7, No. 2, 1969, pp. 279–285.

[2] Chen, P. C., and Liu, D. D., "Harmonic Gradient Method for Unsteady Supersonic Flow Calculations," *Journal of Aircraft*, Vol. 22, No. 5, 1985, pp. 371–379.

[3] Irwin, C. A., and Guyett, P. R., "The Subcritical Response and Flutter of a Swept Wing Model," Royal Aircraft Establishment, Rept. 65186, Farnborough, England, U.K., Aug. 1965.

[4] Hassig, H. J., "An Approximate True Damping Solution of the Flutter Equation by Determinant Iteration," *Journal of Aircraft*, Vol. 8, No. 11, 1971, pp. 885–889.

[5] Rodden, W. P., Harder, R. L., and Billinger, E. D., "Aeroelastic Addition to NASTRAN," NASA CR 3094, March 1979.

[6] Rodden, W. P., *Handbook of Aeroelastic Analysis*, Ver. 65, Vol. 1, MSC/NASTRAN, The MacNeal-Schwendler Corp., Los Angeles, 1987.

[7] Chen, P. C., "Damping Perturbation Method for Flutter Solution: The g-Method," *AIAA Journal*, Vol. 38, No. 9, 2000, pp. 1519–1524.

[8] Karpel, M., "Design for Active Flutter Suppression and Gust Alleviation Using State-Space Aeroelastic Modeling," *Journal of Aircraft*, Vol. 19, No. 3, 1982, pp. 221–227.

[9] Karpel, M., "Time-Domain Aeroservoelastic Modeling Using Weighted Unsteady Aerodynamic Forces," *Journal of Guidance, Control, and Dynamics*, Vol. 13, No. 1, 1990, pp. 30–37.

[10] *ZAERO Version 5.2 Theoretical Manual*, ZONA 01-24.4, ZONA Technology, Inc., Scottsdale, AZ, Nov. 2003.

[11] Adams, W. M., Jr., Tiffany, S. H., Newsom, J. R., and Peele, E. L., "STABCAR—A Program for Finding Characteristic Roots of Systems Having Transcendental Stability Matrices," NASA TP-2165, June 1984.